"A Cochlear Nucleus Auditory prosthesis based on microstimulation"

Contract No. **No. NO1-DC-4-0005**
Progress Report #7

HUNTINGTON MEDICAL RESEARCH INSTITUTES
NEURAL ENGINEERING LABORATORY
734 Fairmount Avenue
Pasadena, California 91105

D.B. McCreery,Ph.D
Leo Bullara, B.S.
Martin Han, Ph.D
A.S. Lossinsky, Ph.D.
V.Pikov ,Ph,D

HOUSE EAR INSTITUTE
2100 WEST THIRD STREET
Los Angeles, California 90057

R.V. Shannon Ph.D
S. Otto M.S.
M. Waring, Ph.D

Introduction

This quarterly report is in three sections.

Part 1 , from HMRI, is a manuscript **"Performance of multisite silicon microprobes chronically implanted in the ventral cochlear nucleus of the cat"** that will be submitted to the IEEE Transactions on Biomedical Engineering, in the first week of May. The manuscript has been reformatted slightly for inclusion in the QPR (Figure captions have been placed immediately below the figures for improved readability, and the title page has been modified). It presents our findings from the animal studies in which multisite silicon probes were implanted chronically in the feline cochlear nucleus. The manuscript includes data from the terminal experiment of one cat (CN155) that has not been reported previously, and also includes a recompilation and an integrated presentation of the raw data from cats CN149, CN152 and CN153, most of which have been reported in previous reports.

Part 2 describes our progress at HMRI towards developing our own silicon substrate probes using the deep reactive ion etching (Deep RIE) process. This will yield mechanically rugged probes that will be suitable for chronic implantation in the feline cochlear nucleus and inferior colliculus, and ultimately, for a clinical prosthesis.

Part 3, from the House Ear Institute, describes recent results from the patients with Type II Neurofibromatosis (NF2), who have been implanted with the arrays of microelectrodes. This section also contains recent data from patients from Dr. V. Colletti's clinical practice in Verona, Italy who have conventional auditory brainstem implants. The goal is to understand the basis for the large differences in performance of the patients with NF2 and those who deafness is from other etiologies.

Part 2

Development of Multi-site Silicon Microelectrodes Arrays at HMRI

We have been developing multisite silicon microelectroprobes for stimulating and recording in the feline cochlear nucleus (CN) and inferior colliculus (ICC).

Recently we have made significant progress in establishing silicon-based probe fabrication technologies at HMRI, using a combination of in-house facilities and facilities rented from the Micromaching Laboratory at the California Institute of technology. The HMRI-silicon probes offer a unique set of capabilities for acute and chronic microstimulating and recording by ***combining*** in a single design, ***all*** of the following :(1) Probe shafts whose thickness can be specified to obtained the required mechanical strength and stiffness for each application (2) multiple recording and stimulation sites on single or multiple shafts (3) conformal insulation over all surfaces of the probes, and (4) probe tips with specified geometry and sharpness to achieve optimal penetration through the pial membrane, while minimizing damage in the underlying brain parenchama .

We have elected to use the deep reactive ion etching (DRIE) technology to form the silicon shafts, and have successfully fabricated probes of various thicknesses, *e.g.*, 50 µm (Figure 1(c)) and 100 µm (Figure 1(d)) with excellent control and uniformity of thicknesses across 4-inch diameter silicon wafers. By repeated polymer deposition and reactive ion etching (Bosch process), the DRIE technology enables fabrication of well-defined vertical wall features (Figure 1(c-d)). The thicknesses of the probe shafts can be controlled, ranging from a few microns to several hundreds microns, by controlling the etching depths on the silicon wafers. This level of flexibility in probe thickness has been unachievable with probes fabricated by the boron etch-stop method, which are limited to a thickness of approximately 15 µm, and we have combine this with advanced photolithographic techniques necessary to produce multiple electrodes sites on a single shaft. These photolithographically-patterned features and the silicon-based shafts are then electrically insulated and protected from dissolution during prolonged exposure to a saline environment, by encapsulating all probe surfaces (top, back and sides) with a conformal coating (Parylene-C). This insulation layer then is ablated from the electrodes sites and bonding pads using an excimer laser. Finally, in order to facilitate the probes' penetration through the pia mater, and to reduce tissue damage within the brain parenchema, we have developed a method to shape their tips in 3 dimensions by a combination of photolithographic patterning and mechanical shaping of the probe tip using mechanical grinding. Furthermore, the taper angle and final tip dimensions (*e.g.*, currently 20°± 5°and 10± 2µm (Figure 1(e)-(f)) c an be varied without changing the photolithographic processing (at the wafer-level), allowing greater flexibility in the probe designs.

Our current mask sets incorporates 2-shank silicon probes for the cat cochlear nucleus (Figure 1) and longer, single-shank probes for the inferior colliculus (Figure 2). We also have fabricated probe of two different thicknesses to compare their suitability for insertion into these two brain structures, without flexing or fracturing.

The wafer-level fabrication processes were conducted in the cleanroom of the Micromaching Laboratory at the California Institute of Technology, while all of the design work and the mechanical shaping of the tip was performed at HMRI.

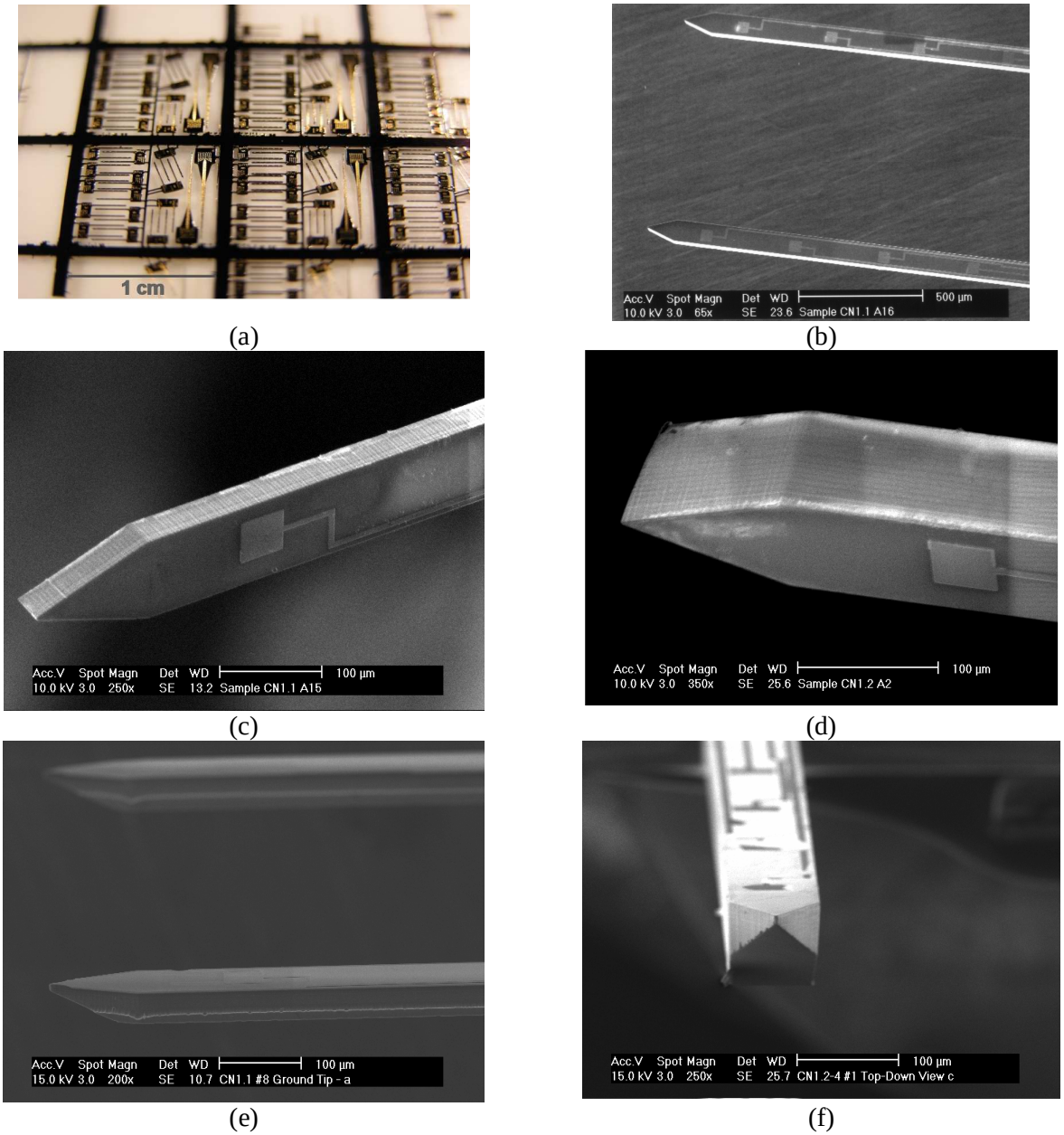

Figure 1: Cochlear nucleus probes fabricated by HMRI. (a) Optical microscopy view of a small portion of a silicon wafer with individual probes before being released out of the wafer, (b) a scanning electron microscopic (SEM) view of a 50 µm-thick probe with two shafts, (c) an enlarged view at the tip of the 50 µm-thick probe before tip-grinding, (d) an enlarged view at the tip of a thicker 100 µm-thick probe before tip-grinding, (e) side-view of ground tips of 50 µm-thick probes, and (f) end-on view of ground tip of 100 µm-thick probes.

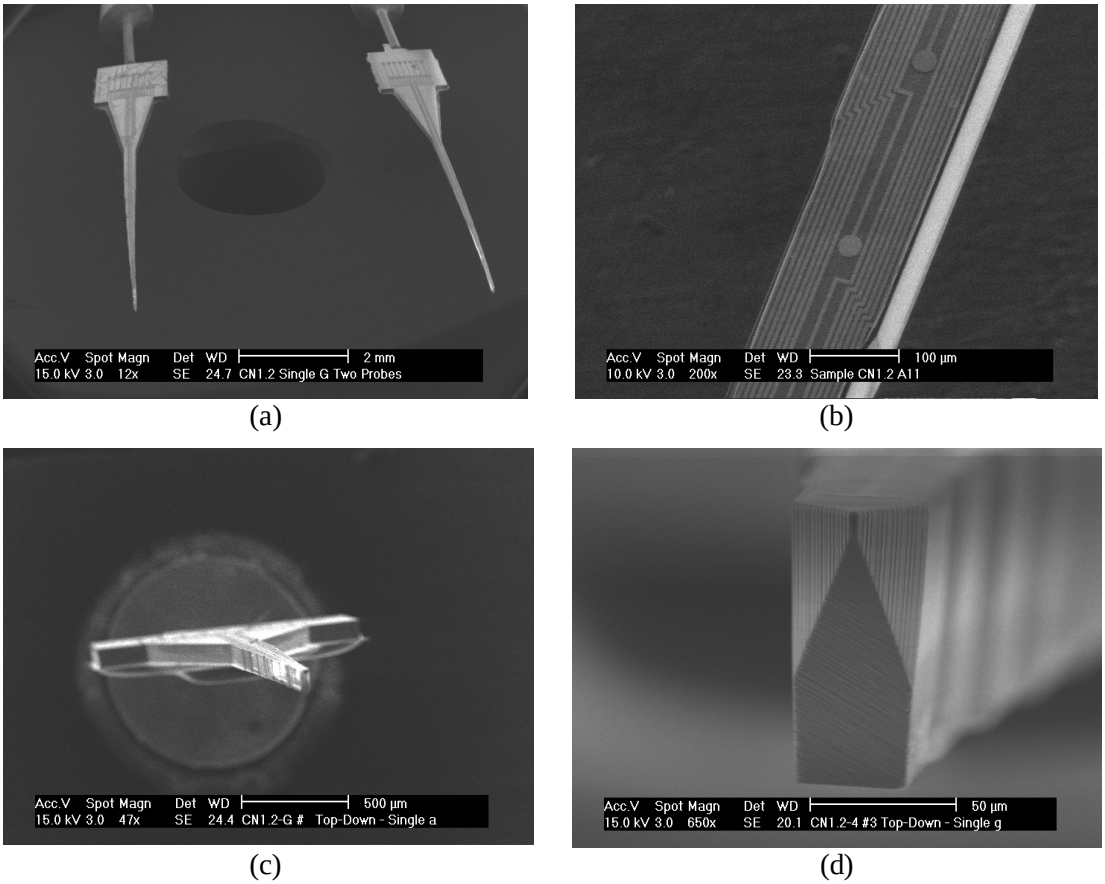

Figure 2: Silicon Inferior Colliculus probes fabricated by HMRI. (a) two long probes, (b) SEM view of a region of a 50 µm-thick silicon shaft, showing metal interconnects (gold/platinum/ titanium), with the smallest line width of 4 µm, and the bases of electrode sites (30 µm in diameter). (c) end-on view of the probe structure with 100 µm-thick thickness, and (d) an enlarged end-on view of the ground tip of 100 µm-thick ICC probe.

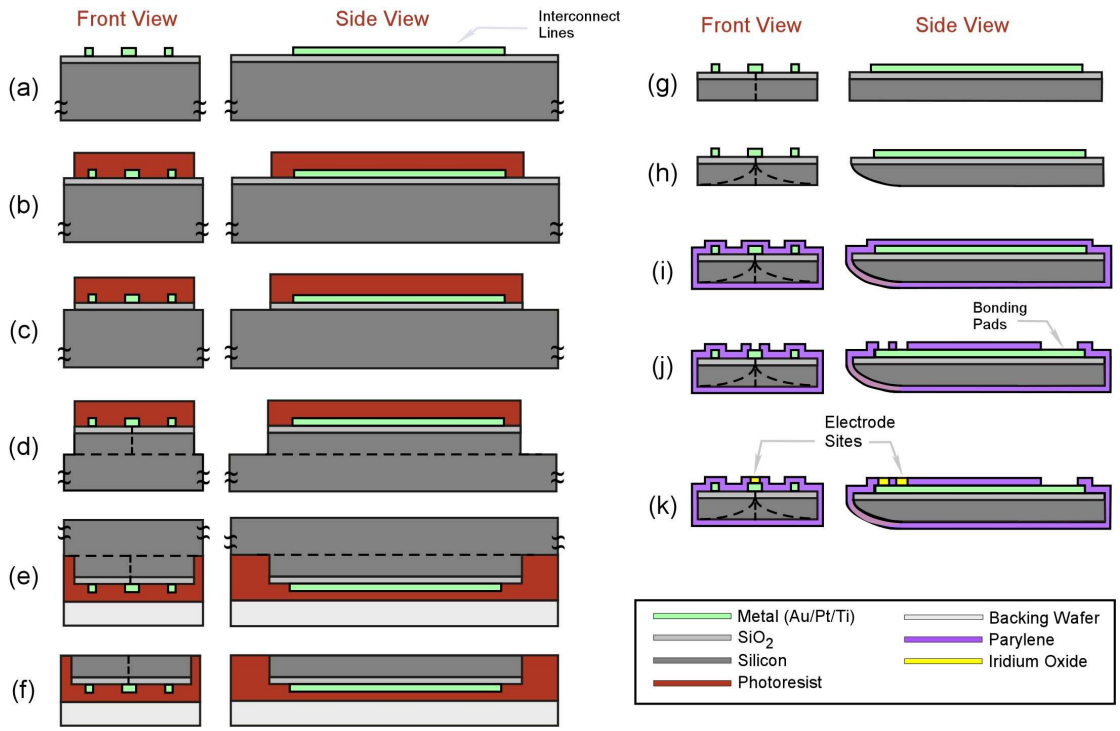

Figure 3: A process flow chart illustrating major steps involved in fabrication of HMRI-silicon probes.

The major wafer-level fabrication steps are illustrated in Figure 3.
(a) On SiO_2-grown silicon wafer, a bilayer of photoresists (AZ 1518 and Lift-Off Resist) is photolithographically patterned to give an undercut wall profile, and evaporation and lift-off of 0.03 µm-thick titanium, 0.03 µm platinum and 0.2 µm gold films, are performed, defining the transmission lines and the bases of active electrodes. (b) A thick photoresist layer (AZ4400) is spun and is patterned to shape the probe structure. (c) Buffered hydrofluoric acid is used to etch the silicon dioxide layer. (d) The top side of the silicon layer is etched anisotropically by deep reactive ion etching (DRIE) for a desired thickness of eventual probe thickness is achieved, *e.g.*, 50 µm or 100 µm. (e) After stripping the existing photoresist layer, another layer of thick photoresist (AZ4620) is spun, and the wafer is flipped and bonded to a backing wafer via oven-baking in order to prepare for back-side DRIE step. (f) DRIE is performed to the backside of the device silicon wafer in order to etch the wafer until the bottom surface of the probe structure is reached (Figure 1(a)). (g) Individual probes are now taken out of the wafer plane and photoresist is subsequently stripped. (h) The tips of the probes are then mechanically ground using a grinding tool (Figure 1(e)-(f)). The shape and dimensions of probe tips can be controlled by using grinding angle and time. (i) All surfaces are then covered with a conformal insulating material Parylene-C. (j) The electrode sites as well as bonding pads are opened using an excimer laser, and Parylene-C residues are cleaned in oxygen plasma etcher. (k) Finally, iridium oxide is electroplated on the active electrode sites.

When etched from the wafer, the probes taper at an angle of about 20° in the plane of the features and in that plane have a radius of curvature the tip of about 2 µm (Figure 1(c)-(d)).

However, in profile the tips have a chisel-like "vertical" edge that must be modified so that the probe can easily penetrate through the pial membrane, yet retain resistance to chipping. The probe is fixed in a spring-loaded jig mounted on a microdrive inclined at the desired angle (22°) above the plane of a grinding wheel and lowered by the microdrive until it contacts the rotating wheel (Figure 4), then advanced by a specified amount. As the process nears completion, the pressure against the wheel decreases and grinding slows and then ceases. The process is very reproducible, so that the probe's thickness at the very tip can be specified accurately (e.g, 10 ± 2 µm) by controlling the grinding time. Figure 1(e)-(f) and Figure 2(c)-(d) show probe tips formed by this method.

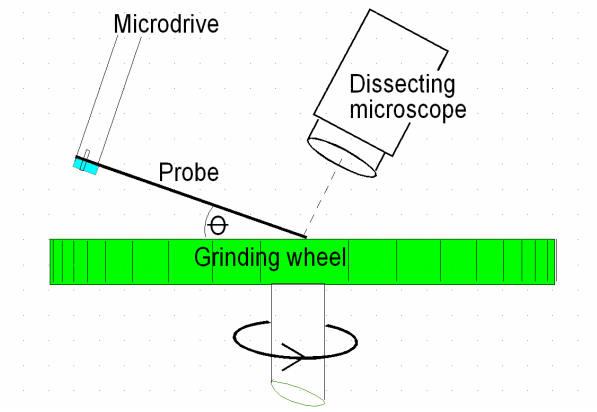

Figure 4.

During the next 2 quarters, we expect to finalize the development of the silicon probes and begin evaluating them *in vitro* and *in vivo*. We expect to complete the following:

- Develop electroplating of iridium oxide (IrOx) onto gold electrode sites to increase charge injection capacities and to lower electrode impedance
- Develop packaging of the probes for acute recording in the ICC, and for chronic implantation in the ICC and the CN
- Conduct *In-vitro* testing of CN and ICC probes (impedance and charge-injection capacity) and begin evaluation long-term stability during soak at room temperature and at elevated temperature. We are awaiting delivery from InnerSea Technologies, Inc of an instrument to detect and track low-level current leakage during soak tests, and we have completed construction of the apparatus that will contain the test samples and maintain them at various temperatures between 37 and 90° C. If found necessary by the accelerated testing, we will deposit another triple-sandwich of SiO_2-SiN_x-SiO_2 dielectric coatings over the metal features before depositing Parylene-C, for better protection against saline intrusion and to improve adhesion of the Parylene.
- Optimize the mechanical probe structure (probe thickness and configuration of the tip region) in acute studies in a cat model.
- Evaluate the recording and stimulation capabilities of the probes in acute experiments in cats
- Begin chronic implantation of CN and ICC probes in cats.

Part 3
Studies conducted at the House Ear Institute

PABI Patients Audiological Measures

Four of the six patients with the penetrating microelectrode array plus the surface auditory brainstem array ("PABI patients") were tested during the first quarter of 2006. PABI patients 1 and 2 were evaluated audiologically as part of their regular follow-up. PABI#3 was tested audiologically and psychophysically. PABI 6 had his initial stimulation and psychophysical testing during this period. One PABI implantation was attempted in January, but an ABI was placed rather than a PABI due to anatomical uncertainties caused by the large tumor. Several potential PABI candidates were evaluated and counseled during this period. Two of them received PABIs in late March. PABI #7 is a middle-aged professional musician now deaf from type II Neurofibromatosis (NF2). PABI #8 is a young woman in her 20's. Both patients will complete their initial stimulation sessions in late May or June, 2006. Two more PABI candidates received initial counseling and evaluation sessions during this reporting period and are now scheduled for implantation in June and July.

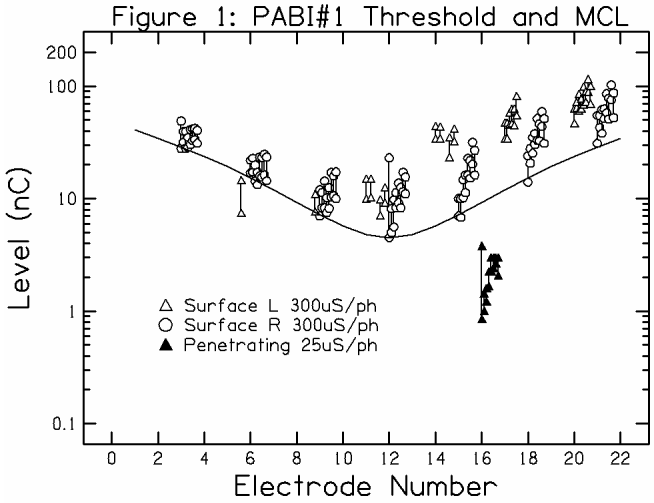

PABI #1 was seen in March 2006 for her 30-month follow-up and still reports hearing on only one penetrating electrode. Threshold and MCL levels were stable as shown in figure 1. Each cluster of data points for each electrode represent sequential measures over time. Each vertical line connects threshold and MCL measures made at the same visit. Points are offset slightly to the right to show any changes in threshold of MCL levels over time. Some electrodes showed slight increase in threshold and MCL over time (12, 15, 18, 21) and some showed stable measures over time (3, 6). Thresholds on the single penetrating electrode (16) that provides auditory sensation increases over the first year but have now been stable for more than one

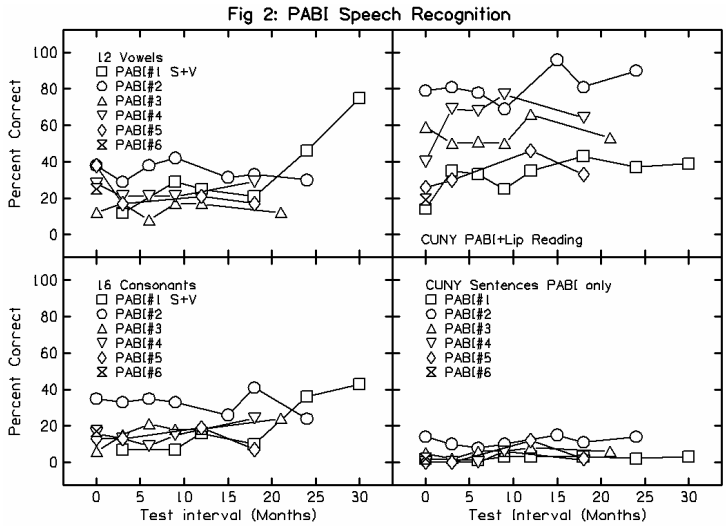

year. PABI#1 reports using her surface or combination map “full-time” (most waking hours) and showed improvement in performance on some speech perception tests this visit (Figure 2). Note the improvement from months18 to 30 in vowel and consonant recognition scores (upper and lower left panels, respectively). Due to her low level of speech recognition performance she has been tested on vowel and consonant recognition in sound (PABI) plus lip-reading mode. All other patients are tested in PABI only mode.

PABI #2 was tested in March 2006 and shows stable performance, preferring and generally performing best with her combination (surface + penetrating electrode) map. She is a full-time (~14 hours per day) user of her PABI. She scores 90% correct in sound-plus-lipreading mode on the CUNY Sentence test (64% with lipreading only). Her speech recognition performance showed no improvement over time (Figure 2). Threshold and MCL measures were are presented in Figure 3. Some threshold levels show a decrease over time (e.g., 3, 6, 9) while most show no change. Penetrating electrodes showed stable thresholds over time.

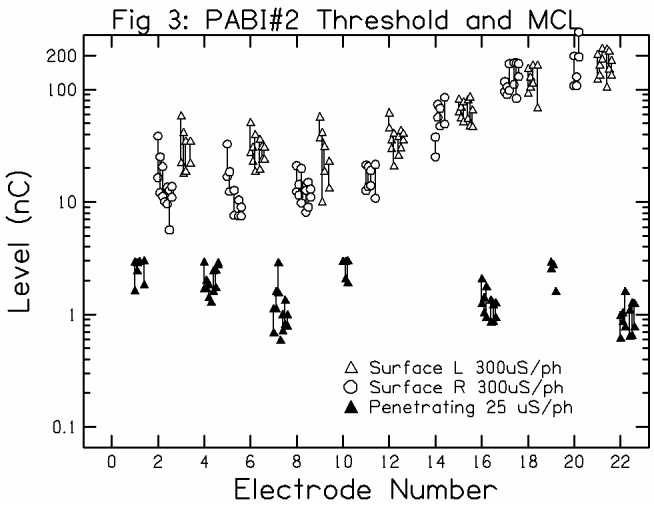

PABI #3 was seen for audiological and psychophysical testing in February 2006. He continues to receive some auditory sensation on 4 of his penetrating electrodes, although the loudness at the charge limit of 3 nC is below the comfort level. His thresholds are quire stable on both surface and penetrating electrodes (Figure 4), with several electrodes showing a decrease over time (9, 12, 18). He is showing stable speech perception performance (Figure 2) and uses his PABI to some degree (mostly the surface-only and surface + penetrating maps) even though he has very good remaining hearing in the other ear.

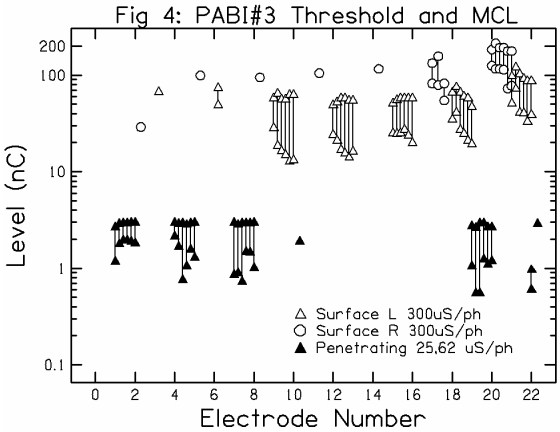

PBBI patients #4 and 5 have never received auditory sensations from their penetrating microelectrodes. Plain x-rays indicated that the penetrating array had dislodged from the brainstem of PABI#4, probably soon after implantation. Intraoperative videos indicate that the penetrating array was implanted medial of the ventral cochlear nucleus in PABI#5.

PABI #6 was seen for initial stimulation in January 2006. He received auditory sensations on 6 of 10 penetrating electrodes, but he experienced only non-auditory sensations on all surface electrodes. He was the first patient to receive the modified PABI electrode array, which includes two additional penetrating electrodes and enlarged surface area on all penetrating electrodes. The charge limit was increased to 8 nC due to the increased surface area. PABI #6 thresholds and MCL levels are presented in Figure 5. Threshold values were below 1 nC/phase for electrodes 13, 16, and 20. All electrodes that produced auditory sensations were located along one half of the penetrating array, with the lowest thresholds observed on the electrode at the edge of the carrier (16). PABI #6 was given a speech processor map using only penetrating electrodes and reports daily use since January. Prior to PABI implantation, he was one of the rare NF2 patients who benefit from a cochlear implant and was an excellent cochlear implant user, indicating that his cochlear nerve and central auditory system was intact up to the time the tumor was removed. However, his vestibular schwannoma grew to the point that it became a health threat and required removal. At the time of initial stimulation PABI 6's speech recognition scores were essentially at chance, with no open set speech recognition (Figure 2).

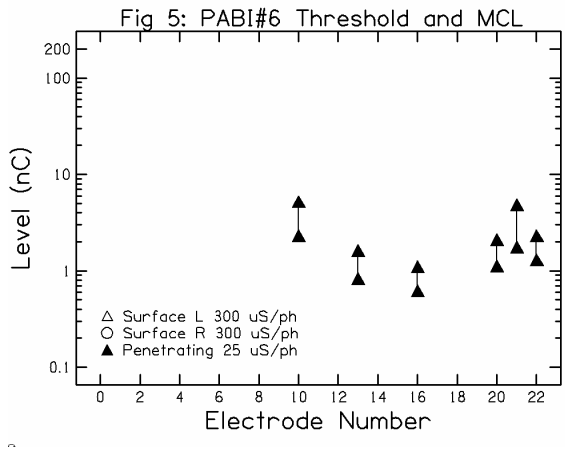

PABI Psychophysics

Psychophysical measures were collected on PABI patients 3 and 6 during this quarter. Pulse rate discrimination was measured in both, while modulation detection and electrode discrimination were also measured in PABI 6.

Figure 6 presents electrode discrimination results from PABI6 at the time of initial activation. Only penetrating electrodes produced auditory sensations in this patient. A set of 6 electrodes was selected and balanced in loudness at a comfortable level. Two electrodes were selected at random and presented to the subject. He was instructed to select the one that was higher in pitch. This process was repeated until all possible pairs of electrodes were presented 20 times. A confusion matrix was constructed and the perceptual distance metric d' was computed for each comparison. Figure 6 plots the cumulative d' measure for

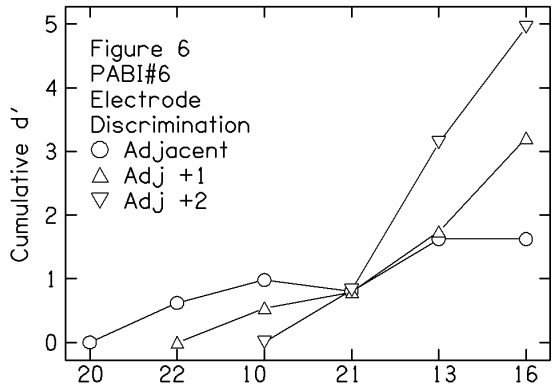

different electrode combinations. The open circles, labeled "Adjacent" shows the d' discriminability measure for adjacent electrodes. The electrodes are ordered along the abscissa approximately in pitch order. The adjacent curve plots the d' value between the electrode listed and the one listed to its left on the abscissa. Across the 6 electrodes only one comparison of adjacent electrodes resulted in a d' of one or more (13 vs 21). The "Adj+1" and "Adj+2 curves plot the cumulative d' for comparisons of electrodes that are separated by 1 or 2 electrodes in terms of pitch. Thus, the curve with inverted triangles plots d' of 21 vs 20, 13 vs 22, and 16 vs 10. These comparisons all result in d' values of one or more, showing good pitch discrimination across this set. The total cumulative d' for the "ADJ+2" set is 5, and is 3.2 for the "Adj+1" set. These values indicate that, although not all pairs of penetrating electrodes produce highly discriminable pitch sensations, many combinations are highly discriminable.

Figure 7 presents modulation detection results from PABI#6. The stimulus was a 400-ms duration, 250-Hz train of biphasic pulses modulated sinusoidally at 10 Hz. Two stimuli were presented and the subject was instructed to select the one with the modulation, or "wobble". The depth of modulation was adaptively adjusted according to a 3-down, 1-up rule to converge on the point of 79% correct. Figure 7 presents results from two penetrating electrodes as a function of the loudness of the carrier stimulus. The modulation threshold is similar for the two electrodes and does not change appreciably over the range of loudness values tested. Modulation detection of -20 dB is equivalent to 10% modulation. Previous results (Fu, 2002; Shannon and Colletti, 2005) show a significant correlation between speech recognition and modulation thresholds, with a modulation threshold of 10% predicting poor speech recognition.

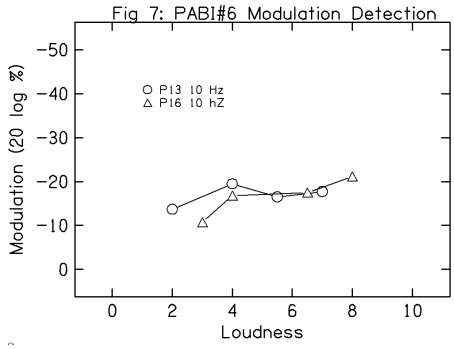

Pulse rate discrimination is another psychophysical task that measures the temporal resolution of implant perception. Two stimuli are presented: a standard stimulation pulse rate and a higher rate. The subject is instructed to select the sound that is higher in pitch and the difference in rate is adaptively changed to measure the 79% correct point. Figure 8 presents the rate discrimination results from PABI 3 and PABI 6 as a function of the standard pulse rate. Results are presented from one penetrating electrode from PABI 6 and from two penetrating and two surface electrodes in PABI 3. Discrimination performance

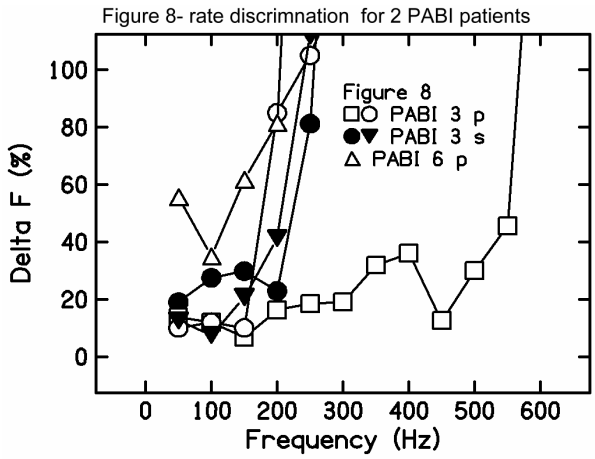

was about 20% for PABI 3 and 40-60% for PABI 6 at low standard pulse rates, but increased to more than 100% as the pulse rate was increased. For 4 of the 8 electrodes tested the frequency at which rate discrimination was lost (exceeded one octave) was 200-250 Hz. One electrode allowed rate discrimination up to 550 Hz in PABI 3. Thus, not only is there a difference in rate discrimination across subjects, but even a large difference across electrodes in the same listener.

ABI Non-NF2 Patients

Two trips were made in this quarter to Verona to test non-NF2 ABI patients with high performance: January and March 2006. Eleven patients were tested in January, including one patient with an implant on the inferior colliculus, and 10 patients were tested in March (3 were the same patients as in January and 7 were new patients). High levels of open set speech recognition have been documented in ABI patients without NF2 tumors. The present psychophysical testing attempts to delineate the basic perceptual differences between NF2 ABI, non-NF2 ABI and PABI performance. Psychophysical testing focused on temporal measures that might be related to the observed differences in speech recognition: temporal integration, pulse phase duration effects (both reported in the previous progress report), pulse rate discrimination, gap detection, and forward masking. In addition, intensity discrimination and electrode discrimination were measured as indicators of intensity and spectral resolution.

Gap detection measures the time of silence between two stimulus bursts that is just detectable. The subject hears two intervals: one contains a continuous 400 ms stimulus and the other contains the same stimulus with a brief silent gap in the middle. The subject is instructed to select which interval contains the gap and the duration of the gap is changed adaptively (3-down, 1-up) to determine the threshold for the gap duration. Figure 9 presents gap detection thresholds as a function of the stimulus loudness for 9 non-tumor ABI patients. The solid line shows average NF2 ABI data from 7 patients, the dashed line shows average gap detection by normal hearing listeners, and the hatched area shows average gap detection by 38 cochlear implant listeners. Filled symbols show data from NT patients with good speech recognition (>50% open set sentence recognition) while open symbols show data from patients with <50% recognition. While there is a tendency for low gap thresholds to go with good speech recognition the sample size is too small to draw definite

Fig 9: Gap Detection

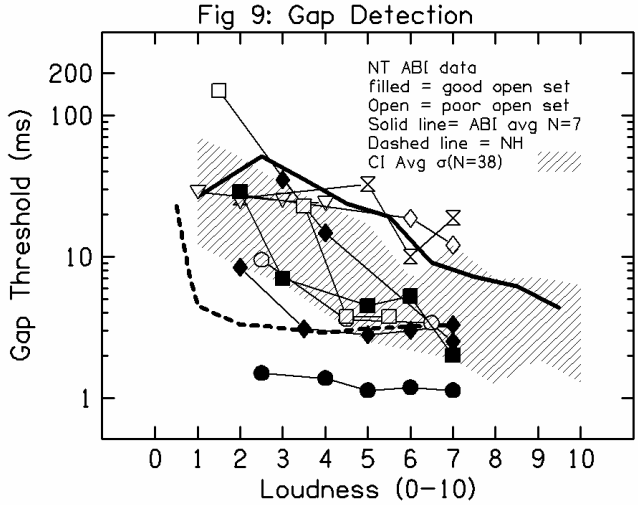

conclusions. Most ABI listeners (both NF2 and non-tumor) are within the range of gap detection thresholds for CI listeners.

Forward Masking measures the residual effect of a prior stimulus over time. A masker is presented at a medium loudness and then turned off. The threshold of a brief signal is measured as a function of the time delay of the signal following the masker offset. Forward masking measures the recovery from adaptation caused by a preceding masker. Figure 10 presents normalized forward masking recovery functions for 3 high-performing non-tumor ABI patients and one NF2 ABI patient (LG). The thick solid line presents forward masking recovery functions for 7 NF2 ABI patients, and the hatched area shows the average functions from 20 cochlear implant subjects. Masking levels were normalized so that the maker level was defined as 100 and the curves were all normalized to a value of 33 at a 200 ms delay (the present experimental program does not allow signal delays longer than 200 ms, so the curves were normalized to the level at 200 ms on the NF2 ABI curves for comparison). It appears that the high-performing non-tumor ABI patients might have a slightly longer recovery time in forward masking than other ABI or CI listeners. Previous studies have shown that the shape of the recovery curves are strongly determined by the loudness functions. If the loudness mapping function is different between NF2 and non-tumor ABI patients (which is unknown at the present time) then that might explain this apparent difference. That is, it is possible that the apparent difference in Figure 10 is not due to a difference in temporal processing but is a reflection of a difference in loudness mapping. Additional measures are needed to resolve this ambiguity.

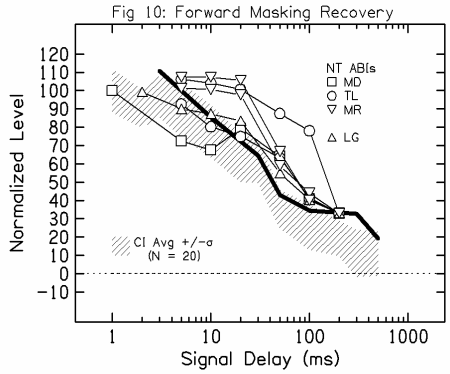

Intensity discrimination measures the smallest change in stimulus intensity that can be detected. Acoustic listeners can typically detect 0.5-1 dB at most listening levels. Cochlear implant listeners can typically detect amplitude changes of 5-10% of the electrical dynamic range. Two sounds are presented to the subject and they are instructed to indicate which sound is louder. The difference in charge in each pulse is then adaptively adjusted by

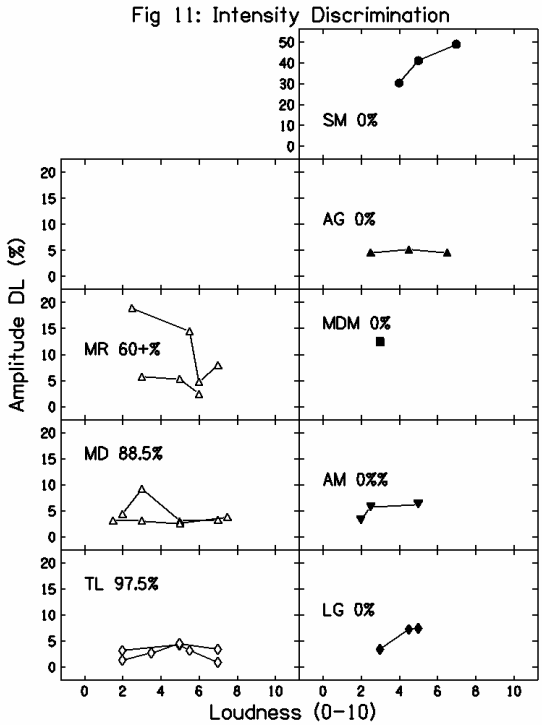

changing the pulse phase duration to measure the point at which they would obtain 79% correct. Figure 11 presents intensity discrimination as a function of the level of the standard stimulus for 6 non-tumor ABI patients and two NF2 ABI patients (LG and SM). Multiple curves in some panels represent measures on two different electrodes. Most patients can detect a change in intensity of 5-15%, but NF2 patient SM was only able to hear changes of 30-50%. The number listed in each panel is the open-set speech recognition score for that listener. Panels on the left show intensity DL measures for patients with good open set speech recognition and panels on the right show results from patients with no open set speech recognition. By inspection there doesn't appear to be a significant difference in intensity discrimination across performance or across etiology, but the sample size is too small to make any definitive conclusions at this time.

Pulse Rate Discrimination measures the smallest change in pulse rate that is detectable at 79% correct using a two-alternative forced-choice procedure. The subject hears two sounds: a standard rate stimulus and another stimulus with a higher pulse rate than the standard. In the present experiment the two stimuli were equal amplitude rather than balanced in loudness or jittered in loudness. Loudness does not change appreciably with pulse rate, so that loudness should not be a confounding cue until standard rates are higher than 300 Hz and the rate discrimination is higher than 50%. If loudness were to effect the results it would improve performance by adding another discriminable dimension, so the present results could be interpreted as a lower bound on rate discrimination *per se* - the actual ability to discriminate stimulation rate may be poorer than these data indicate. Figure 12 presents pulse rate discrimination results from 10 patients: nine non-NF2 ABI patients and results from PABI#3. The number in each panel presents the open set speech recognition for that patient. Note that most patients can detect pulse rate differences of 10-20% up to base frequencies of 250-300 Hz. The transition from good rate discrimination to poor is quite rapid, in some cases going from less than 20% to more than 100% within 50 Hz change in the base rate. From this small sample it does not appear that there is a correlation between pulse rate discrimination and speech recognition performance or etiology. PABI#3 shows good rate discrimination up to a high base frequency,

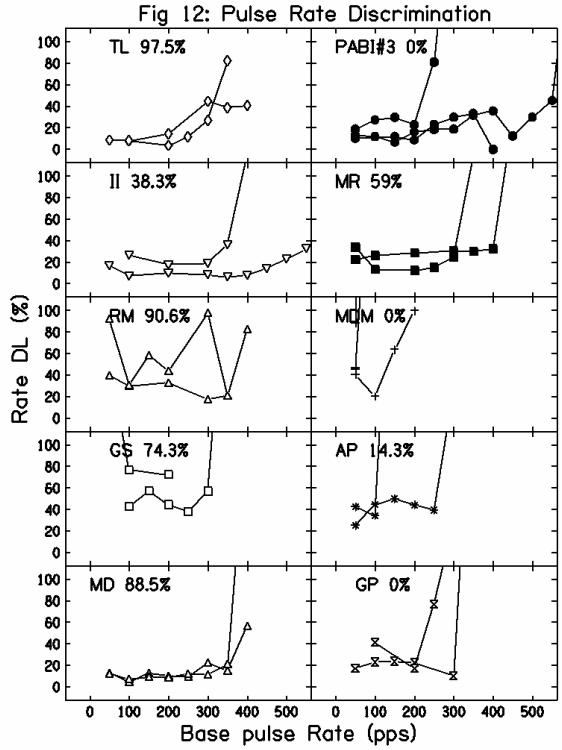

yet get no open set speech understanding. Subject GS, who gets 74.3% open set speech recognition requires 40% change in base rate for detection.

Electrode discrimination was also measured on 8 non-NF2 subjects in this quarter but the data are not fully analyzed at this time. A full analysis will be presented in the next quarterly report.